PCCP

Accepted Manuscript

ROYAL SOCIETY OF CHEMISTRY

www.rsc.org/pccp

New Insights into the Ideal Adsorbed Solution Theory

Sylwester Furmaniak[1], Stanisław Koter[2], Artur P. Terzyk[1,*], Piotr A. Gauden[1], Piotr Kowalczyk[3], Gerhard Rychlicki[1]

[1] *Physicochemistry of Carbon Materials Research Group, Department of Chemistry, N. Copernicus University, 7 Gagarin St. 87- 100 Toruń, Poland*

[2] *Faculty of Physical Chemistry, Department of Chemistry, N. Copernicus University, 7 Gagarin St. 87 - 100 Toruń, Poland*

[3] *School of Engineering and Information Technology, Murdoch University, Murdoch 6150 WA, Australia*

(*) corresponding author

Artur P. Terzyk

N. Copernicus University

Physicochemistry of Carbon Materials Research Group

Department of Chemistry

Gagarina St. 7

87-100 Toruń

Poland

e-mail: aterzyk@chem.umk.pl

url: http://www.chem.umk.pl/~aterzyk/

tel. (+48) (56) 611-43-71

fax: (+48) (56) 654-24-77

Abstract

GCMC technique is used for simulation of CO_2/CH_4, CO_2/N_2 and CH_4/N_2 mixtures adsorption (at 298 K) on six porous carbon models. Next we formulate a new condition of the IAS concept application, showing that our simulated data obey this condition. Calculated deviations between IAS predictions and simulation results increase with the rise in pressure as in the real experiment. For weakly adsorbed mixture component the deviation from IAS predictions is higher, especially when its content in the gas mixture is low, and this is in agreement with the experimental data. Calculated activity coefficients have similar plots to deviations between IAS and simulations, moreover obtained from simulated data activity coefficients are similar qualitatively as well as quantitatively to experimental data. Since the physical interpretation of activity coefficients is completely lacking we show for the first time, that they can be described by the formulas derived from the expression for G^{ex} for the ternary mixture. Finally we also for the first time show the linear relationship between the chemical potentials of nonideal and ideal solutions and the reduced temperature of interacting mixture components, and it is proved that the deviation from ideality is larger if adsorption occurs in more microporous system.

Graphical abstract

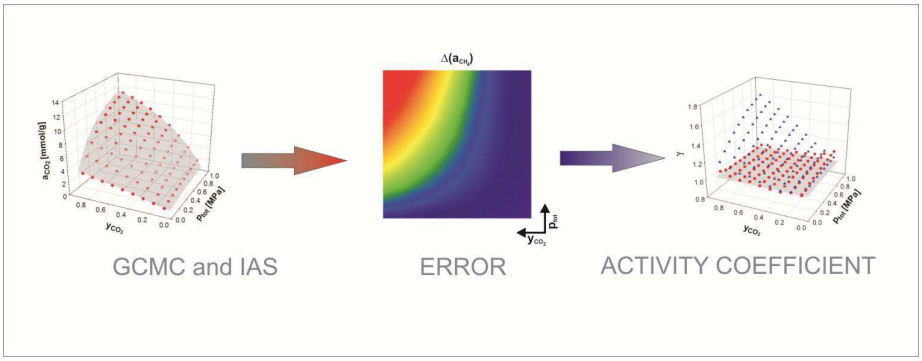

Keywords: Adsorption, Mixture adsorption, GCMC simulation, IAS, theory, thermodynamics of adsorption, activity coefficient

1. Introduction

Developed in 1965 by Myers and Prausnitz the Ideal Adsorbed Solution (IAS) approach[1] is still used for prediction of mixture gas adsorption from single components adsorption isotherms,[2] as well as for description of mixtures adsorption from gaseous phase and even from solutions.[3-8] Moreover the IAS is also capable to predict adsorption from ternary gas mixtures.[9] The most practical application of this concept is probably the calculation of selectivity,[10-12] however, it should be remembered that the extensive computational study of Monsalvo and Shapiro[13] proved that the selectivity coefficients calculated from the IAS can deviate from experimental (deviations in the range of 35-45 %) thus the IAS estimations should be treated with care.

It was widely proved that in many cases the agreement exists between measured experimentally and calculated theoretically (using IAS concept) adsorption isotherms. Thus for example for the mixture of ethane and ethylene adsorbed on 13X molecular sieves, mixture isotherms were measured and the results were compared with the IAS predictions showing excellent agreement.[14] Similar situation occurs, for example, for methane/ethane mixtures adsorbed on the BPL carbon.[15] There is also agreement between simulated and calculated by IAS isotherms. Thus, for example, a good agreement was observed for GCMC and IAS calculated selectivity coefficients of Xe/Kr mixture in zeolite NaA.[16] IAS theory also predicts well the GCMC data of binary mixtures of hydrocarbons adsorption (methane, ethane and propane) in the zeolite silicalite,[17] propane/propylene isotherms on CuBTC MOF,[18] methane, nitrogen and propane mixtures adsorbed on MCM-41 and nanotubes,[19] methane/ethane mixtures on porous carbon model (with exception of high pressures),[20] methane, ethane, propane, n- and isobutane adsorbed in silicalite-1,[21] CO_2/N_2, CO_2/CH_4 and CH_4/N_2 adsorbed in ZIFs,[22] CH_4/H_2 on different IRMOFs,[23] O_2/N_2 mixture in C_{168} Schwarzite,[24] methane/ethane mixtures on MCM-41, CO_2/N_2 and CH_4/N_2 in MOFs and zeolites,[25] CO_2/CH_4 mixtures in pores of activated carbon[26,27] etc.

Considering the basic assumptions of the IAS it is obvious that this theory predicts well selectivity at low loadings, for the gases having similar molecular volumes, and if the molecules adsorbed do not interact strongly, and the adsorbate-adsorbent system is not too heterogeneous.[28,29] For this reason, for example, the deviations between the IAS predictions and GCMC results were smaller for the system Xe-Kr (similar dimensions of molecules) than for Xe-Ar (for adsorption on zeolite NaA).[16] Also since adsorption capacities of p-xylene (8 molecules/unit cell) and toluene (also 8 molecules/unit cell) are different in PARA silicalite

than the capacity for m-xylene (6 molecules/unit cell) the IAS predictions are in fact no so good (comparing to the GCMC results) for p-xylene/m-xylene and m-xylene/toluene mixtures. Contrary for p-xylene/toluene mixture on PARA silicalite, IAS works very well due to similar adsorption capacities of components.[30]

In the subject of selectivity predicted by the IAS model a very interesting paper has been published recently by de Oliviera et al.[31] The authors pointed out the importance of the fact that the pore size distribution (PSD) of components in a mixture can be different than the PSD of individual components, and they proposed a simple mixing rule, assuming that the "contribution" of individual PSD curves to the global adsorption is proportional to the molar fraction of components in the gas phase. Calculated, taking this into account, selectivity can be remarkably different than that obtained from the IAS concept.

It was also proved that the IAS model applied for calculation of the composite binary mixture isotherm from the singe component isotherms does not predict the data adequately if the so called "segregation effect" occurs.[32] It was also shown that for adsorption of the mixtures of CO_2, N_2 and H_2 in zeolite Na-4A IAS predicts that the adsorption selectivity is essentially independent on the gas phase composition.[33] However, the GCMC results show that the selectivity decreases markedly as the gas phase mole fraction of CO_2 in the gas mixture increases (note that at 1.0 atm the overprediction of IAS selectivity estimation is 70 %). Thus in this case IAS results are accurate only at low CO_2 pressures.[33]

The IAS predictions strongly depend on the choice of isotherm model applied for the description of single component adsorption isotherms.[7,12,33-38] To avoid this Chen and Sholl[39] developed the transition matrix Monte Carlo (TMMC) approach but it can be applied only for simulated and not for experimental adsorption data.

As it can be concluded from the short introduction presented above, there is a lack of systematic and complex studies on the IAS concept. Certainly this concept is valid since it has strong thermodynamic basis, however during calculation of binary isotherms and selectivity coefficients the fundamental assumption of the IAS approach, i.e. that the solution should be "ideal", is often forgotten. Since the IAS assumes ideality it works well only up to the particular pressure limit. There are attempts in literature to take nonideality of solution into account. Thus for example, Li et al.[40] used Real Adsorption Solution Theory (RAST) introducing activity coefficients from the Wilson's theory using the method proposed earlier by van der Vaart et al.[41] However, as it was pointed out by van der Vaart et al.[41] themselves, the Wilson interaction parameters are not only completely different from those found for bulk solutions, but also the physical interpretation of these parameter values is completely lacking.

Thus some new solutions in this field should be found. And this is the next purpose of our study.

Therefore, we check the applicability of IAS for description of binary mixtures isotherms calculated for adsorption on realistic, so called "Virtual Porous Carbon" (VPC) models proposed recently.[42] Since in real systems it is not simple to achieve systematic and controlled changes in porosity and/or in chemical composition of surface layer, we use molecular simulations. The application of VPC offers also complete knowledge about the pore size distributions (PSD) of applied VPC. This is very important information since chemical composition of carbon surface layer and porosity determine adsorption properties of activated carbons. Summing up, using the VPC and GCMC simulations we are able to generate a series of single and multicomponent adsorption isotherms and next, to use the IAS concept for the description of simulation results. In this way we are able to relate the characteristics of carbons with the range of IAS applicability, we can calculate errors and activity coefficients and finally we can try to relate the values of activity coefficients with some physicochemical characteristics of carbon models. Since we base on VPC our studies are limited to activated carbons and not necessary are valid for other adsorbents.

2. Calculation details

2.1 Simulation boxes

In this work, we use three virtual porous carbon (VPCs) models denoted as d0.5, d0.9 and d1.3 which were described in details previously.[42] They were generated following the simple Metropolis Monte Carlo method employing one of the most sophisticated carbon force fields, i.e. the environment-dependent interaction potential for carbon (EDIP) proposed by Marks.[43,44] Additionally, basing on the d0.9 carbon the series of three gradually oxidized structures was generated using the previously proposed virtual oxidation procedure.[45] For simplicity, only carbonyl groups are investigated (as it was shown by Jorge et al.,[46] who considered water adsorption, the type of oxygen-containing group is not of critical importance, since more complex groups can effectively be represented by simpler sites; a similar conclusion was also provided by Di Biase and Sarkisov[47] who studied the adsorption of CO_2 and CH_4). The following numbers of carbonyl oxygen atoms were introduced: 52, 104 and 156. These oxidised VPCs were denoted as d0.9_052, d.0.9_104 and d0.9_156. All the model carbons (presented schematically on Fig. 1) were placed in a cubicoid simulation box

having dimensions 4.5×4.5×4.5 nm with periodic boundary conditions in all three directions. The porosity of the studied carbonaceous adsorbents was characterised by a geometrical method proposed by Bhattacharya and Gubbins (BG).[48] The implementation of the method was described in details elsewhere.[42]

2.2 Monte Carlo simulations

Due to practical importance[50-53] we consider three binary gas mixtures: CO_2/CH_4, CO_2/N_2 and CH_4/N_2. Their adsorption at 298 K on the above described model carbons was simulated using grand canonical Monte Carlo method (GCMC).[54,55] The simulations were performed for the following values of total pressure (p_{tot}): 0.1, 0.2, 0.3, 0.4, 0.5, 0.6, 0.7, 0.8, 0.9, and 1.0 MPa and for each pressure value different mole fractions of components in gaseous phase (y) were assumed, i.e. 0.1, 0.2, 0.3, 0.4, 0.5, 0.6, 0.7, 0.8, and 0.9. The methodology of calculations was analogical as that described previously.[56] Each GCMC simulation run consists of 2.5×10^8 iterations. The first 1.0×10^8 iterations are discarded to guarantee equilibration. One iteration is an attempt of the system state change by the randomly selected perturbation: (i) displacement and/or rotation of randomly chosen molecule, (ii) creation of new molecule, (iii) annihilation of randomly chosen existing molecule or (iv) swap move with equal probabilities. We use equal probability for each perturbation to guarantee the condition of microscopic reversibility. Both the adsorbent structure and the molecules of adsorbate are modelled as rigid ones. Tab. 1 collects all the applied values of the interaction parameters. The Lorentz-Berthelot mixing rules are used for calculation of cross-term energy parameters (with the exception of the C-H interaction between different CH_4 molecules – see Tab. 1 and ref. 58).

From the GCMC simulation results, we determine the average numbers of each kind of adsorbate molecules in the simulation box ($\langle i \rangle$). These values are used for calculation the absolute adsorption amounts of each component per unit of adsorbent mass (a_i) ant their mole fractions in adsorbed phase (x_i). Finally, in order to illustrate the efficiency of mixture separation we also compute the values of equilibrium separation factors:

$$S_{1/2} = \frac{x_1/x_2}{y_1/y_2} \tag{1}$$

The adsorbed phase is enriched in the 1st component if $S_{1/2} > 1$.

Similarly (i.e. using analogical Monte Carlo simulation scheme), adsorption isotherms of pure gases (i.e. CO_2, CH_4 and N_2) are also obtained. We consider the following pressure ranges: 1.0×10^{-6}-1.0 MPa for CO_2, 1.0×10^{-6}-25.0 MPa for CH_4 and 1.0×10^{-6}-60.0 MPa for N_2.

2.3 Thermodynamic background

The thermodynamic background of mixed-gas adsorption and theory of ideal adsorbed solution (IAS) was developed by Myers and Prausnitz[1] in 1965. It was based on the spreading pressure concept associated with adsorption at planar solid-fluid interfaces. For porous adsorbents, as in our case, the thermodynamic formalism was worked out by Myers and Monson.[60] According to both approaches the Gibbs adsorption isotherm for a binary mixture can be expressed as (Eq. (20) in ref. 1, Eq. (3.16) in ref. 60):

$$d\psi = a_1 d\ln f_1 + a_2 d\ln f_2 \tag{2}$$

where a_i, f_i are the specific absolute adsorption, the fugacity of i-th component, respectively, ψ is the reduced grand potential. In the case of flat adsorbent surfaces[1] it is defined as:

$$\psi = \frac{A\pi}{RT} \tag{3}$$

where π is the spreading pressure, A is the specific surface area of adsorbent, T is absolute temperature and R is the universal gas constant. For porous adsorbents the definition of ψ is:[60]

$$\psi = -\frac{\Omega}{RT} \tag{4}$$

where Ω is the grand potential (here it is divided by the mass of adsorbent):

$$\Omega = F - \sum_i a_i \mu_i = \mu_s - p_{tot} v_s \tag{5}$$

In Eq. (5) F is the specific Helmholtz free energy of solid phase, μ_i is the chemical potential of i-th adsorbate in the solid phase equal in equilibrium to its chemical potential in the gas

phase, μ_s is the chemical potential of solid adsorbent, p_{tot} is pressure in the gas phase and v_s is the specific volume of solid phase.

We can also obtain Eq. (2) from the Gibbs-Duhem equation written for the pore volume of our adsorbent (the difference between the volume of simulation box and the volume of adsorbent) as (T = const.):

$$\sum_i a_i d\mu_{i,p} - v_p dp_p = 0 \tag{6}$$

Here v_p is the pore volume divided by the adsorbent mass, $\mu_{i,p}$ is the chemical potential of i-th adsorbate in the pore volume equal in equilibrium to its chemical potential in the gas phase and p_p is pressure inside the pores. From Eq. (6) Eq. (2) results with that difference that now ψ is defined as:

$$\psi \equiv \frac{v_p p_p}{RT} \tag{7}$$

Comparing to Eq. (3) it is seen that A and π are replaced by v_p and p_p, respectively. p_p is a resultant of p_{tot} and the interactions of adsorbates and adsorbent.

One should also mention about another thermodynamic approach of the gas adsorption in a porous solid developed by Talu.[61] According to this approach the grand potential (φ) is defined as (Eq. (16) in ref. 61):

$$\varphi = \mu_s - \mu_s^* = -RT \int_0^{p_i} \sum_i \left(\frac{a_i}{p_i} - \frac{v_s}{RT} \right) dp_i \tag{8}$$

where μ_s^* is the chemical potential of pure adsorbent at $p = 0$. For the absolute adsorption v_s in the above equations is equal to the sum of the inaccessible solid volume and the pore volume (Eq. (36) in ref. 61). In our case v_s is the volume of the simulation box for which the average numbers of adsorbate molecules were determined (see section 2.1). Analysing Eq. (8) it should be noted that as v_s does not depend on p, with the increase of p the value of φ at first will go towards more negative values and then its absolute value will start to decrease, as it is

illustrated in Fig. 2 for a pure gas. As φ has the same value for two different pressures it cannot be regarded as the appropriate definition of the grand potential.

The basic point in the adsorption solution theory is to determine the grand potential. For our case the total pressure (p_{tot}) does not exceed 1 MPa. Therefore, we assume that f_i can be replaced by the partial pressure (p_i). Thus Eq. (2) can be written as:

$$d\psi = \frac{a_1}{p_1}dp_1 + \frac{a_2}{p_2}dp_2 = \left(\frac{a_1 + a_2}{p_{tot}}\right)dp_{tot} + \left(\frac{a_1}{y_1} - \frac{a_2}{y_2}\right)dy_1 \tag{9}$$

where p_i is related to p_{tot} by:

$$p_i = y_i p_{tot} \tag{10}$$

y_i is mole fraction of the i-th adsorbate in the gas phase. Having experimentally (or by simulation) determined a_1 and a_2 for the mixture as a function of p_1 and p_2 (or p_{tot} and y_1), ψ can be determined from Eq. (9) in different ways and each way should give the same value of ψ, because ψ is the state function/variable. E.g. choosing p_1 and p_2 as independent variables, ψ calculated as:

$$\psi(\mathrm{I}) = \int_0^{p_1} \frac{a_1(p_1, p_2 = 0)}{p_1}dp_1 + \int_0^{p_2} \frac{a_2(p_1, p_2)}{p_2}dp_2 \tag{11}$$

should be equal to that obtained from:

$$\psi(\mathrm{II}) = \int_0^{p_2} \frac{a_2(p_1 = 0, p_2)}{p_2}dp_2 + \int_0^{p_1} \frac{a_1(p_1, p_2)}{p_1}dp_1 \tag{12}$$

To fulfil this condition, the equality of mixed partials $\left(\partial\left(\partial\psi/\partial p_1\right)_{p_2}/\partial p_2\right)_{p_1} = \left(\partial\left(\partial\psi/\partial p_2\right)_{p_1}/\partial p_1\right)_{p_2}$ should be satisfied, i.e.:

$$\left(\frac{\partial(a_1/p_1)}{\partial p_2}\right)_{p_1} = \left(\frac{\partial(a_2/p_2)}{\partial p_1}\right)_{p_2} \tag{13}$$

or

$$\left(\frac{\partial\left(\left(a_1+a_2\right)/p\right)}{\partial y_1}\right)_p=\left(\frac{\partial\left(a_1/y_1-a_2/y_2\right)}{\partial p}\right)_{y_1} \tag{14}$$

Eqs. (13) and (14) result from the fact that according to Eq. (9) $\left(\partial\psi/\partial p_1\right)_{p_2}=a_1/p_1$ and $\left(\partial\psi/\partial p_2\right)_{p_1}=a_2/p_2$. Checking of these equalities is very important – if they are not fulfilled it means that the results are not accurate or the theory expressed by Eq. (9) does not hold for a given system. It should be stated that up to our knowledge no such tests were published till now in the papers reporting the results of the IAS concept.

For the mixing process carried out at constant grand potential ψ and T the two equalities hold:

$$\psi=\psi_1^{\mathrm{o}}=\psi_2^{\mathrm{o}} \tag{15}$$

where ψ_i^{o} refers to ψ in the single gas adsorption and is given by Eq. (9) written for that case:

$$\psi_i^o=\int_0^{p_i^o}\frac{a_i^o}{p}dp \tag{16}$$

From the equality of chemical potentials of adsorbate in the gas phase and in the adsorbate solution it results that the pressure of a pure *i*-th component corresponding to ψ and p_i^o, is given by (Eqs. (5.4) in ref. 60 and (25) in ref. 61 for the ideal gas phase):

$$p_i^o=\frac{p_i}{\gamma_i x_i}=\frac{y_i p_{tot}}{\gamma_i x_i} \tag{17}$$

where p_i is the partial pressure of *i* in the gas mixture, x_i and γ_i are the mole fraction and the activity coefficient of the *i*-th component in the adsorbed solution, respectively.

In the case of IAS it is assumed that $\gamma_i = 1$ and only the second equality of Eq. (15) (i.e. $\psi_1^o = \psi_2^o$) is taken into account. Thus, from Eqs. (15)-(17) x_i as a function of y_i and p_i is obtained. For ψ the total amount of adsorbed gases (a) is given by (Eq. (4.14) in ref. 60):

$$a = \frac{1}{x_1/a_1^o + x_2/a_2^o} \tag{18}$$

where a_i^o is the amount of adsorbed i-th component in absence of another component calculated for the same ψ. The amount of i-th component adsorbed from the mixture (a_i) is calculated from:

$$a_i = x_i a \tag{19}$$

In the case of nonideal adsorption solutions the activity coefficients γ_1 and γ_2 are calculated from the equalities (15) taking the experimental (in our case determined from the GCMC simulation) values of x_i.

2.4. Checking of equality of ψ(I) and ψ(II)

We tested the consistency of our data by comparing ψ(I) with ψ(II) calculated from Eqs. (11) and (12). In those calculations a_1/p_1 and a_2/p_2, obtained from the direct simulation of binary mixtures adsorption, were approximated independently as a function of p_1 and p_2 by the empirical function:

$$g_i(p_1, p_2) = \sum_{k=1}^{N} \frac{a_{m,i,k} K_{a,i,k}}{1 + \left(K_{a,i,k} p_i\right)^{n_{i,k}} + \left(K_{a,ij,k} p_j\right)^{n_{ij,k}}} \qquad i \neq j = 1,2 \tag{20}$$

where $g_i = a_i/p_i$, $K_{a,i,k}$, $n_{i,k}$ and $n_{ij,k}$ are the best-fit parameters (not negative), N (usually 2 or 3) was chosen to obtain a good fit ($R^2 > 0.9999$). Among other tested functions Eq. (20) gave the best fit. It should be noted that Eq.(20) is not symmetric, i.e. $\partial g_1 / \partial p_2 \neq \partial g_2 / \partial p_1$ (see Eq. (13)) even in the case of a very good fit. Therefore, when this function is used one should

expect smaller or higher differences between ψ(I) and ψ(II). On the other hand, the use of a function with a symmetry property would have no sense.

The smallest deviation of ψ(I) (Eq. (11) from ψ(II) (Eq. (12)) was observed for the carbon d0.5 (0.13-1.2 %), the highest deviation for the systems: d0.9_104 and adsorption of CO_2/N_2 mixture (11 %) and d0.9 and CH_4/N_2 mixture (10 %), although the fit quality for those systems was very high ($R^2 > 0.99996$). No regularity was observed, e.g. for the system d0.9_156 and CH_4/N_2 mixture only 0.16 % deviation was observed. Thus generally we can conclude that the simulation adsorption results can be described by Eq. (9).

2.5. IAS calculations

To find x_1 from the second part of equalities (15) and Eqs. (16) and (17) the single-component isotherms should be approximated by some mathematical equation. In this work, we used (as previously – see ref. 62) the three-modal Bradley's equation in the form:

$$a_i^o\left(p_i^o\right) = \sum_{k=1}^{3} \frac{a_{m,i,k}\left(K_{i,k}\,p_i^o\right)^{n_{i,k}}}{1+\left(K_{i,k}\,p_i^o\right)^{n_{i,k}}} \tag{21}$$

where $a_{m,i}$, K_i, and n_i are the best-fit parameters. During the fitting isotherms by Eq. (21), we minimised the mean relative error (*MRE*):

$$MRE = \frac{1}{NP}\sum_{i=1}^{NP}\left|\frac{a_{apr,i}-a_{sim,i}}{a_{sim,i}}\right|\times 100\% \tag{22}$$

where *NP* is the number of points of a simulated isotherm, $a_{apr,i}$ and $a_{sim,i}$ are the approximated by Eq. (21) and simulated adsorption amount for *i*-th point, respectively. Obtained values of the best-fit parameters are collected in Tab. S1 in ESI. As one can see, in the case of the considered simulated adsorption isotherms of pure CO_2, CH_4 and N_2, *MRE* does not exceed 0.5 %.

It should be noted that for the gas which is less adsorbed $p_i^o(\psi)$ is always higher than that for the more adsorbed gas, as it results from Eq. (16). The gas mixture pressure corresponding to the same ψ is between these two pressures. In our case we have found that

the pressure of less adsorbed gas can be much higher (even 30 times) than that of the mixture pressure. Therefore the adsorption of CH_4 and N_2 were simulated also for high pressure values. Substituting Eq. (21) into Eq. (16) we get:

$$\psi_i^{\circ} = \sum_{k=1}^{3} \frac{a_{m,k}}{n_k} \ln\left(1 + \left(K_k p_i^o\right)^{n_k}\right) \tag{23}$$

Taking into account Eq. (17) with $\gamma_i = 1$, x_1 was found by solving the second part of equalities (15). Having x_1 at the equilibrium, we calculated the equilibrium separation factor ($S_{i/j}$) from Eq. (1) and the adsorption amounts of components (a_i) from Eq. (19).

In order to illustrate the differences between the predictions of IAS theory and the results of direct simulation of mixtures adsorption for each considered point (defined by the combination of p_{tot} and y_1 values) we calculated the relative "errors" of the components adsorption amounts and equilibrium separation factors:

$$\Delta\left(q\left(p_{tot}, y_1\right)\right) = \frac{\left|q_{IAS}\left(p_{tot}, y_1\right) - q_{sim}\left(p_{tot}, y_1\right)\right|}{q_{sim}\left(p_{tot}, y_1\right)} \times 100\% \tag{24}$$

where q denotes the considered quantity (a_i or $S_{1/2}$) and subscripts "IAS" and "sim" relate to the values obtained from IAS theory and from the simulations, respectively.

2.6. The activity coefficients of components in the adsorbate solution

The observed deviations between the IAS prediction and the "experimental" (simulated) adsorption from the gas mixture can be attributed to the nonideal behaviour of adsorbates in the "adsorbate solution". The nonideal behaviour of the gas mixture is of minor importance because the pressure was not high (≤ 1 MPa).

The activity coefficients γ_1 and γ_2 of the components of adsorbate solution were calculated by solving the equalities (15) with the substituted Eqs. (16) and (17) (x_1 was taken from the simulation experiment). To reduce the approximation errors, we calculated ψ for the mixture not from Eq. (11) or (12) but using the equation:

$$\psi = \int_0^{p_{tot}} \frac{a_1 + a_2}{p} dp \qquad y_1 = \text{const.} \tag{25}$$

Thus, two approximations ($a_i/p_i = g_i(p_1,p_2)$, i = 1, 2) in the whole experimental range of p_1 and p_2, were replaced by the approximations $(a_1+a_2)/p = g(p)$ for each value of y_1 (equal to 0.1, 0.2, …, 0.9). It was found that the functions:

$$g(p) = \frac{b_1 + b_2 p^{b_3}}{b_4 + p^{b_3}} \tag{26}$$

or

$$g(p) = \frac{b_1 + b_2 p}{1 + b_3 p + b_4 p^2} \tag{27}$$

are useful for that purpose (b_1-b_4 are the best-fit parameters). To analyze the dependencies $\gamma_1(x_1)$ and $\gamma_2(x_1)$ at constant ψ they were calculated as follows. For a given value of y_1 (p_{tot} is a variable) we approximated x_1, γ_1 and γ_2 as a function of ψ using the function:

$$z = \left(\frac{\psi}{c_1}\right)^{c_2} \exp(c_3 \psi) \tag{28}$$

where $z = x_1$, γ_1 or γ_2 and c_1-c_3 are the best-fit parameters. In most cases, Eq. (28) worked satisfactorily. Next x_1, γ_1, γ_2 were calculated from Eq. (28) for a given ψ chosen from the range common for all y_1 values: $\psi_{min}(y_1=0.9)$, $\psi_{max}(y_1=0.1)$. The obtained set of 9 points was finally approximated by the existing formulas relating γ_i with x_i.

3. Results and discussion

Fig. 3 shows the BG pore size distribution curves of studied VPC samples. One can observe that all the studied samples are strictly microporous (pores with d_{eff} below 2 nm). The distribution of microporosity is the widest for the sample d0.5, and the narrowest for d1.3. It is also important, that the virtual oxidation procedure does not change the geometric PSD

curve remarkably, and for the samples d0.9, d0.9_052, d0.9_104 and d0.9_156 we observe practically the same PSD.

In Fig. 4 we compare the simulated single component adsorption isotherms (T = 298 K) of studied gases on all the VPC models. As one can see, for all the studied carbons adsorption decreases in the following order: CO_2<CH_4<N_2. The narrowing of pores and shifting of the PSD toward smaller pore diameters (see Fig. 3) leads to progressive changes in the shapes of simulated adsorption isotherms, i.e. isotherms from linear (i.e. Henry's type) become more characteristic to the Type I.

The IAS predictions were based only on the grand potential ψ^o for pure gases calculated from Eq. (23). As it was mentioned above (Fig. 2) the Talu's grand potential φ^o can show an extremum. Fig. S1 in ESI presents the comparison of φ^o for all the simulated single gas adsorption isotherms. Here φ^o is plotted in the pressure range which results from the condition φ^o(gas 1) = φ^o(gas 2). The minima of $\varphi^o = f(p)$ are clearly seen in the case of N_2 adsorption on all the considered carbons and also of CH_4 adsorption on d1.3 structure. In Fig. 5 ψ^o and φ^o for CO_2 and N_2 versus x_{CO2} are shown in the range close to the simulated value of x_{CO2}. The intersection point determines x_{CO2} according to the IAS theory. It is seen that φ^o used as the grand potential yields in some cases two or no solution depending on the gas mixture composition (y_{CO2}). This is the reason why further in the text we discuss only the results based on ψ defined according to the Myers and Monson formalism.

The results comparing IAS predictions and simulations are collected in Fig. 6 (for d0.9 carbon) and Figs S2-S6 in ESI (for other carbons). One can see that for all the systems adsorption values of better adsorbed compound are predicted by the IAS concept very well (we call the better adsorbed compound i.e. CO_2 for CO_2/CH_4 and CO_2/N_2 and CH_4 for CH_4/N_2 mixtures as the 1st one). In contrast, reverse situation is observed for weakly adsorbed compound (called as the 2nd one). The differences between the results of simulation and the IAS predictions increase with the rise in total pressure and the mole fraction of the first component in the gas phase. Similar behaviour (increasing differences between simulation results and the IAS predictions with the rise in p_{tot} and y_1) are observed in the case of equilibrium separation factors.

To compare the differences between the IAS and simulations we calculate the average errors (collected in Fig. 7) of a_1, a_2 and $S_{1/2}$. The errors were averaged for each total pressure value in two groups: for the low mole fraction of the 1st component ($y_1 < 0.5$) and for high y_1 values ($y_1 \geq 0.5$). The analysis of the data from Fig. 7 shows that the errors generally increase

with the rise in pressure. Moreover, the error of equilibrium separation factors calculated by using the IAS is mainly caused by problems in calculation of the second component adsorption. The errors for those two values are similar and (independently from the total pressure) distinctly higher at larger mole fractions of the first component in the gas phase. Regarding the mixtures the deviations decrease in order: CO_2/CH_4, CO_2/N_2, CH_4/N_2. For the second component the deviation is higher, especially when its content in the gas mixture is low. This observation is in agreement with experimental data published by Harlick and Tezel,[63] who concluded that when one component of a mixture is strongly adsorbed and the other component is weakly adsorbed, theoretical models (among them the IAS) do not predict the adsorption behaviour of the weakly adsorbed component well. One can also see that the highest deviations are observed for d0.9 and its modified forms (d0.9_052, d0.9_104, d0.9_156). The modification of d0.9 practically has no effect on the deviation.

It is obvious that the values of errors can correlate with activity coefficients. The plots $\gamma_i = f(p, y_1)$ for all the systems can be found in Fig. 8 (for raw carbons) and in Fig. S7 in ESI (oxidised carbons). They are similar to the deviations. As an example in Fig. 9 we show the dependence between the average relative errors for adsorption of the weakly adsorbed compound (IAS calculation) and the average values of $RT \ln \gamma_2$.

Before we discuss the activity coefficients calculated from the simulated data we present an example showing that the plots of activity coefficients calculated from GCMC are realistic. In Fig. 10 the comparison of our simulated data for CO_2/CH_4 mixture at constant gas mixture pressure (p_{tot} = 0.5 MPa, T = 298 K) with those obtained experimentally by Buss[64] for activated carbon A35/4 at similar pressure (p_{tot} = 0.53 MPa, T = 293 and 313 K) is shown. It is seen that the magnitudes of γ_{CO2} and γ_{CH4} on x_{CO2} are similar. The most similar to experimental data, quantitative as well as qualitative dependence of γ_{CO2} and γ_{CH4} on x_{CO2} is found for d0.9 carbon. According to Buss data[64] the temperature effect on γ_i is insignificant. It should be noted here that more correctly is to compare activity coefficients at constant ψ which is the state variable for the adsorbate solution, not pressure. However, there are no such data in the Buss's work. This example shows that for this case simulation data are very similar to the real ones. However, not for all the carbons the changes of γ with x are the same as shown in Fig. 10. This is seen while analysing another set of calculated γ_i for the CO_2/CH_4 adsorption on micro-porous Norit RB1 activated carbon found in ref. 41. The dependence of γ_{CO2} and γ_{CH4} on x_{CO2} at the constant ψ (ψ = 3, 4 and 5 mmol/g) is shown on Fig. 7 in ref. 41. The nature of dependence is different than ours (Fig. 11 and Figs S8 and S9 in ESI).

Moreover, in our case the influence of ψ on $\gamma_i(x_{CO2})$ is observed, whereas in the case of ref. 41 there is no such influence (with one exception γ_{CH4} for x_{CO2} = ca. 0.9).

In both cited above papers the authors additionally applied the Wilson equation for a binary mixture to fit the activity coefficients. However, as it was pointed out by van der Vaart et al.[41] the Wilson interaction parameters are not only completely different from those found for bulk solutions, but also the physical interpretation of these parameter values is completely lacking. Thus some new solutions in this field should be found. Surprisingly the fit of activity data at constant ψ failed[41] whereas those at constant p were fitted satisfactorily[64]– probably it is a coincidence. However, as Myers pointed out,[65] the use of Wilson equation is justified only at ψ = const, because only in that case one gets $x_1 d\ln\gamma_1 + x_2 d\ln\gamma_2 = 0$ – the basis for Wilson's equation derivation.

Another dependence of γ_i on T, ψ and x_j was proposed by Siperstein and Myers.[66] However, at T,ψ = const it reduces to the one constant Margules equation ($\ln\gamma_i \sim x_j^2$). Such equation gives mirror images of γ_1 and γ_2 and for the liquid mixtures is valid only for the similar components.

Thus, for description of our data we have tried the two-constant Margules equations:[67]

$$\ln\gamma_1 = (A+3B)(1-x_1)^2 - 4B(1-x_1)^3 \tag{29}$$

$$\ln\gamma_2 = (A-3B)x_1^2 + 4Bx_1^3 \tag{30}$$

where A and B are parameters of the Redlich-Kister expansion of the molar excess Gibbs free enthalpy of the two component mixture:[67]

$$\frac{G^{ex}}{RT} = x_1 x_2 \left(A + B(x_1 - x_2) + C(x_1 - x_2)^2 + ...\right) \tag{31}$$

Here A and B are the expansion parameters. Unfortunately, it is not possible to fit our data with Eqs. (29) and (30). However, it is not surprising that the equations elaborated for the binary liquid mixtures do not work – in such mixtures interactions between components 1 and 2 of the type: 1-1, 1-2 and 2-2 occur. In the adsorbate solutions also the interactions with adsorbent i.e.: 1-*adsorbent* and 2-*adsorbent* are present. Thus, we postulate that more suitable

are equations developed for the ternary liquid mixtures. For the adsorbate solution the third constituent would be the vacancies on the surface. However, they cannot be treated as a full constituent. For example, taking into account Eq. (26) from ref. 1 the term x_3 / a_3^o would have to appear. For vacancies the quantity a_3^o does not exist. Therefore we still treat the adsorbate solution as the binary mixture but somehow we have to introduce the interactions of gases with the adsorbent. The simplest way it seems to take just the expression for G^{ex} for the ternary mixture. Following this, two expansions of G^{ex} for the ternary system were tested.

The first one is the extension of Eq. (31) in the following way:

$$\frac{G^{ex}}{RT} = x_1 x_2 \left(A_{12} + B_{12}\left(x_1 - x_2\right)\right) + x_1 x_3 \left(A_{13} + B_{13}\left(x_1 - x_3\right)\right) + x_2 x_3 \left(A_{23} + B_{23}\left(x_2 - x_3\right)\right) \tag{32}$$

The second one is the truncated formula:[68]

$$\frac{G^{ex}}{RT} = x_1 x_2 \left(x_1 A_{21} + x_2 A_{12}\right) + x_1 x_3 \left(x_1 A_{31} + x_3 A_{13}\right) + x_2 x_3 \left(x_2 A_{32} + x_3 A_{23}\right) \tag{33}$$

In Eqs. (32) and (33) the parameters A_{ik} are not the same. The $\ln \gamma_i$ is given by the partial derivative of G^{ex}: $\ln \gamma_i = \left(\partial\left(nG^{ex}/RT\right)/\partial n_i\right)_{T,\psi,n_{j\neq i}}$, where $n = n_1 + n_2 + n_3$. Thus we get:

a) from Eq. (32):

$$\begin{aligned}\ln \gamma_1 = &-x_1 x_2 \left(A_{12} - 2B_{12}\left(1 + x_2 - x_1\right)\right) - x_1 x_3 \left(A_{13} - 2B_{13}\left(1 + x_3 - x_1\right)\right) + \\ &+ x_2 \left(A_{12} - x_2 B_{12}\right) + x_3 \left(A_{13} - x_3 B_{13}\right) - x_2 x_3 \left(A_{23} + 2B_{23}\left(x_2 - x_3\right)\right)\end{aligned} \tag{34}$$

$$\begin{aligned}\ln \gamma_2 = &-x_1 x_2 \left(A_{12} + 2B_{12}\left(1 + x_2 - x_1\right)\right) - x_2 x_3 \left(A_{23} - 2B_{23}\left(1 + x_3 - x_2\right)\right) + \\ &+ x_1 \left(A_{12} + x_1 B_{12}\right) + x_3 \left(A_{23} - x_3 B_{23}\right) - x_1 x_3 \left(A_{13} + 2B_{13}\left(x_1 - x_3\right)\right)\end{aligned} \tag{35}$$

b) from Eq. (33):

$$\ln \gamma_1 = x_2^2 \left(A_{12}\left(1 - 2x_1\right) - 2A_{32} x_3\right) + x_3^2 \left(A_{13}\left(1 - 2x_1\right) - 2A_{23} x_2\right) + 2\left(1 - x_1\right) x_1 \left(A_{21} x_2 + A_{31} x_3\right) \tag{36}$$

Here $\ln \gamma_2$ is obtained from Eq. (36) by exchanging subscripts 1 with 2.

It can be noticed that the above activity coefficients satisfy the condition $\lim_{x_i \to 1} \gamma_i = 1$, whereas we should not expect that the limit of γ_i at $\psi \to 0$ is 1 because of the presence of the 3rd component (adsorbent). The condition $\sum_i x_i d \ln \gamma_i = 0$ is satisfied if we take into account the 3rd component.

To avoid some ambiguities in determining the maximum concentration of vacancies, a_{max}, needed for the calculation of molar ratios in the ternary system we decided to treat a_{max} as a fitting parameter. Thus, x_3 was expressed as $x_3 = 1 - (a_1 + a_2)/a_{max}$, whereas x_1 and x_2 were replaced by x_i for the binary mixture, $x_i(bin) = a_i/(a_1 + a_2)$, using the relation: $x_i = x_i(bin)(1 - x_3)$, i = 1, 2; $x_i(2)$ was calculated as $x_i = a_i/(a_1+a_2)$.

For both assumed G^{ex} expansions the fit is sufficiently good. In the case of G^{ex} given by Eq. (32) the changes of a_{max} are smaller than in the case of Eq. (33) (Tab. S2 in ESI) probably because we have excluded the parameter B_{12} (B_{12} = 0), which had no influence on the quality of the fit. However, it was also found that a_{max} can be changed in a wide range and this change does not influence the quality of the fit. It means that the parameters of the model are strongly correlated. The optimal values of a_{max} seem to be reasonable, because they are higher than the maximum of (a_1+a_2) obtained for the gas mixtures or a_i obtained for pure gases at the highest investigated pressure. Finally, since as it was mentioned by different authors, the physical interpretation of activity coefficients is not simple and sometimes even completely lacking, we try to relate activity coefficients with physicochemical properties of interacting molecules. The correlation between average ln γ_1 or ln γ_2 and the function of critical temperatures $(T_{C1} \times T_{C2})^{1/2}/T$ (where T is the temperature of adsorption) is shown in Fig. 12.

The explanation of the origin of this correlation can be as follows. Empirical combining laws relating the force constants (collision diameters σ and energy of interaction ε) between molecules 1 and 2 can be given as follows:[69]

$$\sigma_{12} = \frac{1}{2}\left(\sigma_{11} + \sigma_{22}\right) \tag{37}$$

$$\varepsilon_{12} = \left(\varepsilon_{11} \times \varepsilon_{22}\right)^{1/2} \tag{38}$$

On the other hand, application of the principle of corresponding states leads to the relation of the type:

$$\varepsilon_i \sim T_{Ci} \tag{39}$$

To take into account that the states of both interacting gases are different we must apply the reduced temperature and finally we can write Eq. (38) in the form:

$$\varepsilon_{12} \sim \frac{\left(T_{C1}T_{C2}\right)^{1/2}}{T} \tag{40}$$

On ordinate of Fig. 12 the difference between the chemical potentials of ideal and real mixture is plotted and the correlation shows that this difference, i.e. the deviation of the system from ideality, depends on the value of the energy of intermolecular interactions between the components of a mixture. It is interesting that for almost all the studied systems (d1.3 is the exception) the strongly adsorbed compound (1st compound in Fig. 12) behaves more ideally than the second mixture component, adsorbed weakly. Thus CH_4 in the mixture with N_2 and CO_2 in the both remaining mixtures are more perfect than N_2 and CH_4. This is caused by the mechanism of adsorption observed on snapshots (not shown). The 1st component behaves more ideally since in this case interactions 1-1 dominate as it is observed for a pure compound. Contrary, component 2 is mainly surrounded by the molecules of component 1 thus 1-2 interactions cause imperfection. The rise in reduced temperature has strong influence on the activity of weakly adsorbed component, and this component in larger extent deviates from ideality than the strongly adsorbed one. It can be also seen that with the shift of the PSD plot (Fig. 3) toward smaller micropores (i.e. from d0.5 down to d1.3) we observe larger deviation from ideality for the both components. In the case of d1.3 carbon with the rise in reduced temperature of the interacting mixture components the deviation from ideality is the largest among all the studied systems; moreover, it is also seen for strongly adsorbed compound. Thus we can conclude, that with the rise in microporosity of carbon the nonideality of adsorbed solution increases.

4. Conclusions

Using GCMC simulations of CO_2/CH_4, CO_2/N_2 and CH_4/N_2 mixtures, adsorption (at 298 K) on six VPC models was studied. The models differ with porosity and with the composition of carbon surface layers (oxygen content). Next, it is shown that the simulated isotherms obey the fundamental condition of IAS application (Eq. (5)). The deviations between IAS predictions and simulation results increase with the rise in pressure. It is also shown that for the second component the deviation from IAS predictions is higher, especially when its content in the gas mixture is low, and this is in agreement with the experimental data published by Harlick and Tezel.[63] Calculated activity coefficients have similar plots to deviations between IAS and simulations. Calculated from simulated data activity coefficients are similar qualitatively as well as quantitatively to experimental data published by Buss.[64] Finally we show that the calculated of activity coefficients can be described by the formulas derived from the expression for G^{ex} for the ternary mixture (Eqs. (32) and (33)). The deviation between chemical potentials of nonideal and ideal solutions increases with the rise in reduced temperature of interacting mixture components, and the deviation from ideality is larger if adsorption occurs in more microporous system.

Acknowledgments

S.F., A.P.T. and P.A.G. acknowledge the use of the computer cluster at Poznań Supercomputing and Networking Centre (Poznań, Poland) as well as the Information and Communication Technology Centre of the Nicolaus Copernicus University (Toruń, Poland). S.F. gratefully acknowledges financial support from *Iuventus Plus* Grant No. IP2012 034872 from the Polish Ministry of Science and Higher Education.

References

1 A. L. Myers and J. M. Prausnitz, *AIChE J.*, 1965, **11**, 121.

2 O. K. Farha, A. M. Spokoyny, B. G. Hauser, Y.-S. Bae, S. E. Brown, R. Q. Snurr, C. A. Mirkin and J.T. Hupp, *Chem. Mater.*, 2009, **21**, 3033.

3 S. J. Allen, G. McKay and J. F. Porter, *J. Colloid Interface Sci.*, 2004, **280**, 322.

4 Z. Yu, S. Peldszus and P. M. Huck, *Water Res.*, 2008, **42**, 2873.

5 Q. Lu and G. A. Sorial, *Carbon*, 2004, **42**, 3133.

6 J. F. Porter, G. McKay and K. H. Choy, *Chem. Eng. Sci.*, 1999, **54**, 5863.

7 J. C. Crittenden, P. Luft, D. W. Hand, J. L. Oravitz, S. W. Loper and M. Arl, *Environ. Sci. Technol.*, 1985, **19**, 1037.

8 D. U. Knappe, Y. Matsui, V. L. Snoeyink, P. Roche, M. J. Prados and M.-M. Bourbigot, *Environ. Sci. Technol.*, 1998, **32**, 1694.

9 B.-M. Jeong, E.-S. Ahn, J.-H. Yun, C.-H. Lee and D.-K. Choi, *Sep. Sci. Technol.*, 2007, **55**, 335.

10 C. Ducrot-Boisgontier, J. Parmentier, A. Faour, J. Patarin and G. D. Pirngruber, *Energy Fuels*, 2010, **24**, 3595.

11 M. R. Hudson, W. L. Queen, J. A. Mason, D. W. Fickel, R. F. Lobo and C. M. Brown, *J. Am. Chem. Soc.*, 2012, **134**, 1970.

12 N. A. Al-Baghli and K. F. Loughlin, *J. Chem. Eng. Data*, 2006, **51**, 248.

13 M. A. Monsalvo and A. A. Shapiro, *Fluid Phase Equilib.*, 2007, **254**, 91

14 R. P. Danner and E. C. F. Choi, *Ind. Eng. Chem. Fundam.*, 1978, **17**, 248.

15 Y. He, J.-H. Yun and N. A. Seaton, *Langmuir*, 2004, **20**, 6668.

16 C. J. Jameson, A. K. Jameson and H.-M. Lim, *J. Chem. Phys.*, 1997, **107**, 4364.

17 M. D. Macedonia and E. J. Maginn, *Fluid Phase Equilib.*, 1999, **158-160**, 19.

18 M. Jorge, N. Lamia and A. E. Rodrigues, *Colloids Surf. A*, 2010, **357**, 27.

19 M. W. Maddox, S. L. Sowers and K. E. Gubbins, *Adsorption*, 1996, **2**, 23.

20 J.-C. Liu and P. A. Monson, *Adsorption*, 2005, **11**, 5.

21 R. Krishna and D. Paschek, *Phys. Chem. Chem. Phys.*, 2001, **3**, 453.

22 B. Liu and B. Smit, *J. Phys. Chem. C*, 2010, **114**, 8515.

23 B. Liu, Q. Yang, C. Xue, C. Zhong, B. Chen, and B. Smit, *J. Phys. Chem. C*, 2008, **112**, 9854.

24 J. Jiang and S. I. Sandler, *Langmuir*, 2003, **19**, 5936.

25 B. Liu and B. Smit, *Langmuir*, 2009, **25**, 5918.

26 P. Billemont, B. Coasne and G. De Weireld, *Adsorption*, 2014, **20**, 453.

27 A. G. Albesa, M. Rafti, J. L. Vicente, H. Sánchez, and P. Húmpola, *Adsorpt. Sci. Technol.*, 2012, **30**, 669.

28 M. Murthi and R.Q. Snurr, *Langmuir*, 2004, **20**, 2489.

29 J. A. Dunne, M. Rao, S. Sircar, R. J. Gorte and A. L. Myers, *Langmuir*, 1997, **13**, 4333.

30 S. Chempath, R. Q. Snurr and J. J. Low, *AIChE J.*, 2004, **50**, 463.

31 J. C. A. de Oliveira, R. B. Rios, R. H. López, H. R. Peixoto, V. Cornette, A. B. Torres, C. L. Cavalcante Jr., D. C. S. Azevedo and G. Zgrablich, *Adsorpt. Sci. Technol.*, 2011, **29**, 651.

32 R. Krishna and J. M. van Baten, *Chem. Phys. Lett.*, 2007, **446**, 344.

33 E. D. Akten, R. Siriwardane and D.S. Sholl, *Energy Fuels*, 2003, **17**, 977.

34 C. R. Clarkson and R. M. Bustin, *Int. J. Coal Geol.*, 2000, **42**, 241.

35 V. Goetz, O. Pupier and A. Guillot, *Adsorption*, 2006, **12**, 55.

36 P. Monneyron, M.-H. Emanero and J.-N. Foussard, *Environ. Sci. Technol.*, 2003, **37**, 2410.

37 R. B. Rios, F. M. Stragliotto, H. R. Peixoto, A. E. B. Torres, M. Bastos-Neto, D. C. S. Azevedo and C. L. Cavalcante Jr., *Braz. J. Chem. Eng.*, 2013, **30**, 939.

38 J. Schell, N. Casas, R. Pini and M. Mazzotti, *Adsorption*, 2012, **18**, 49.

39 H. Chen and D. S. Sholl, *Langmuir*, 2007, **23**, 6431.

40 M. Li, E. Xu, T. Wang and J. Liu, *Langmuir*, 2012, **28**, 2582.

41 R. van der Vaart, C. Huiskes, H. Bosch and T. Reith, *Adsorption*, 2000, **6**, 311.

42 S. Furmaniak, *Comput. Methods Sci. Technol.*, 2013, **19**, 47.

43 N. A. Marks, *Phys. Rev. B*, 2000, **63**, 035401.

44 N. Marks, *J. Phys.: Condens. Matter*, 2002, **14**, 2901.

45 S. Furmaniak, A. P. Terzyk, P. A. Gauden, P. J. F. Harris and P. Kowalczyk, *J. Phys.: Condens. Matter*, 2009, **21**, 315005.

46 M. Jorge, Ch. Schumacher and N. A. Seaton, *Langmuir*, 2002, **18**, 9296.

47 E. Di Biase and L. Sarkisov, *Carbon*, 2013, **64**, 262.

48 S. Bhattacharya and K. E. Gubbins, *Langmuir*, 2006, **22**, 7726.

49 W. Humphrey, A. Dalke and K. Schulten, *J. Mol. Graphics*, 1996, **14**, 33.

50 M. Ricaurte, C. Dicharry, D. Broseta, X. Renaud and J. P. Torre, *Ind. Engn. Chem. Res.*, 2013, **52**, 899.

51 Y. S. Bae, K. L. Mulfort, H. Frost, P. Ryan, S. Punnathanam, L. J. Broadbelt, J. T. Hupp and R. Q. Snur, *Langmuir*, 2008, **24**, 8592.

52 M. P. Bernal, J. Coronas, M. Menéndez and J. Santamaria, *AIChE J.*, 2004, **50**, 127.

53 Q. Yang, L. Ma, C. Zhong , X. An and D. Liu, *J. Phys. Chem. C*, 2011, **115**, 2790.

54 D. Frenkel and B. Smit, *Understanding Molecular Simulations*, Academic Press, New York, 2002.

55 E. Tylianakis and G. E. Froudakis, *J. Comput. Theor. Nanosci.*, 2009, **6**, 335.

56 S. Furmaniak, P. Kowalczyk, A. P. Terzyk, P. A. Gauden and P. J. F. Harris, *J. Colloid Interface Sci.*, 2013, **397**, 144.

57 T. X. Nguyen, PhD Thesis, University of Queensland, Brisbane, 2006.

58 A. P. Terzyk, S. Furmaniak, P. A. Gauden and P. Kowalczyk, *Adsorpt. Sci. Technol.*, 2009, **27**, 281.

59 J. J. Potoff and J.I. Siepmann, *AIChE J.*, 2001, **47**, 1676.

60 A. L. Myers and P. A. Monson, *Adsorption*, 2014, **20**, 591.

61 O. Talu, *J. Phys. Chem. C*, 2013, **117**, 13059.

62 S. Furmaniak, A. P. Terzyk, K. Kaneko, P. A. Gauden, P. Kowalczyk and T. Ohba, *Chem. Phys. Lett.*, 2014, **595-596**, 67.

63 P. J. E. Harlick and F.H. Tezel, *Sep. Purif. Technol.*, 2003, **33**, 199.

64 E. Buss, *Gas Sep. Purif.*, 1995, **9**, 189.

65 A. L. Myers, *AIChE J.*, 1983, **29**, 691.

66 F. R. Siperstein and A. L. Myers, *AIChE J.*, 2001, **47**, 1141.

67 S. I. Sandler, *Chemical and Engineering Thermodynamics*, Wiley, New York, 1999.

68 W. H. Severns Jr., A. Sesonske, R. H. Perry and R.L. Pigford, *AIChE J.*, 1955, **1**, 401.

69 J. O. Hirschfelder, C. F. Curtiss and R. B. Bird, *Molecular Theory of Gases and Liquids*, Willy and Sons, New York, 1954.

Table 1

The values of LJ potential parameters and point charges applied in simulations

	Geometric parameters	Centre	σ [nm]	ε/k_B [K]	q/e	Reference
CO_2	$l_{C=O}$ = 0.1162 nm	C	0.2824	28.680	+ 0.664	57
		O	0.3026	82.000	– 0.332	
CH_4	$l_{C–H}$ = 0.1090 nm $\Theta_{H–C–H}$ = 109.5°	C	0.3400	55.055	– 0.660	58
		H	0.2650	7.901	+ 0.165	
		C-H[a)]	0.3025	30.600	–	
N_2	$l_{N\equiv N}$ = 0.1100 nm	N	0.3310	36.000	– 0.482	59
		COM[b)]	–	–	+ 0.964	
VPC	$l_{C=O}$ = 0.1233 nm	C[c)]	0.3400	28.000	–	46
		C[d)]	0.3400	28.000	+ 0.500	
		O	0.2960	105.800	– 0.500	

[a)] cross-interaction parameters

[b)] centre of mass

[c)] non-carbonyl group atom of C

[d)] carbonyl group C atom

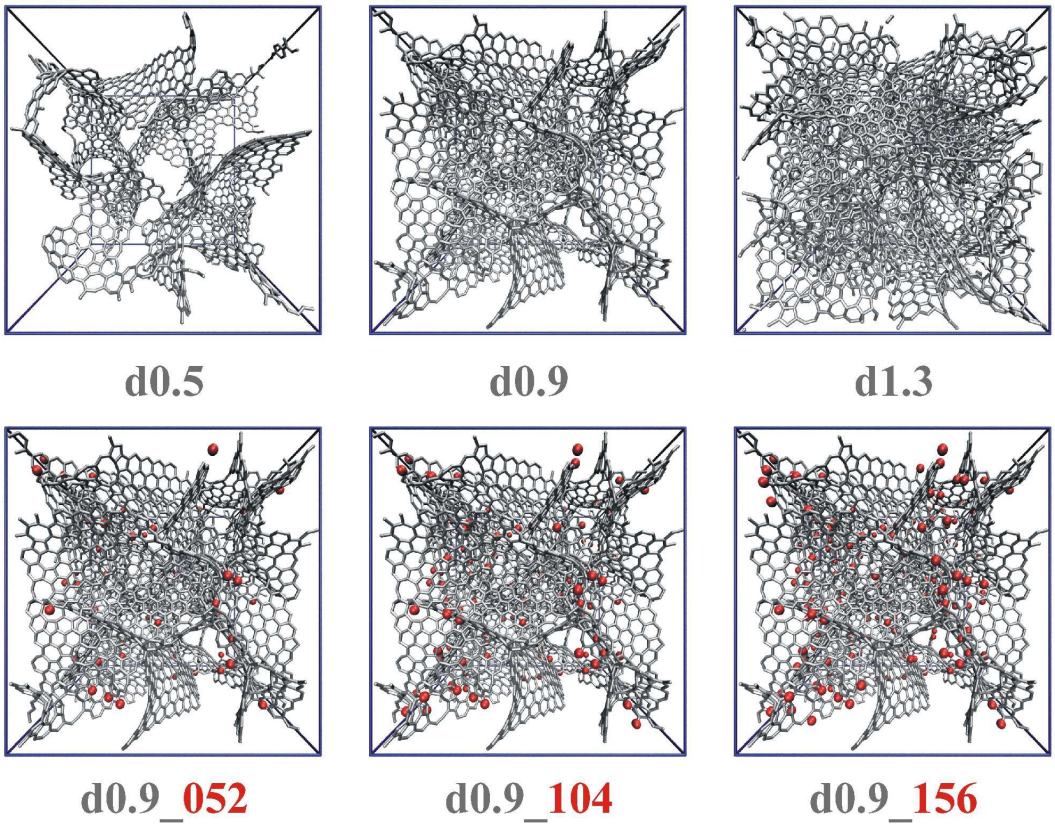

Figure 1. Schematic representation of all the considered VPCs (oxygen atoms are marked as the red balls; the frames reflect the size of the simulation box). It should be noted that this figure was created using the VMD program.[49]

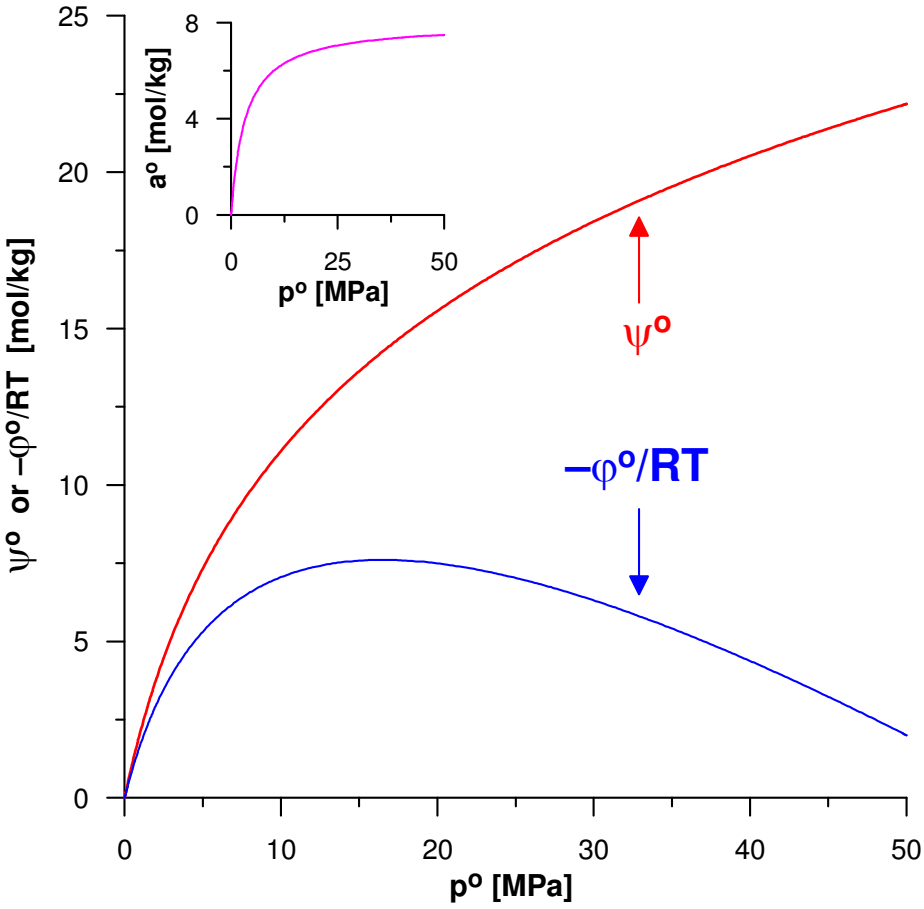

Figure 2. Comparison of grand potentials ψº (Eq. (16)) and φº (Eq. (8)) calculated for arbitrarily generated single gas adsorption isotherm at T = 298 K (inset); during the φº calculation we assumed v_s = 0.001 m^3/kg.

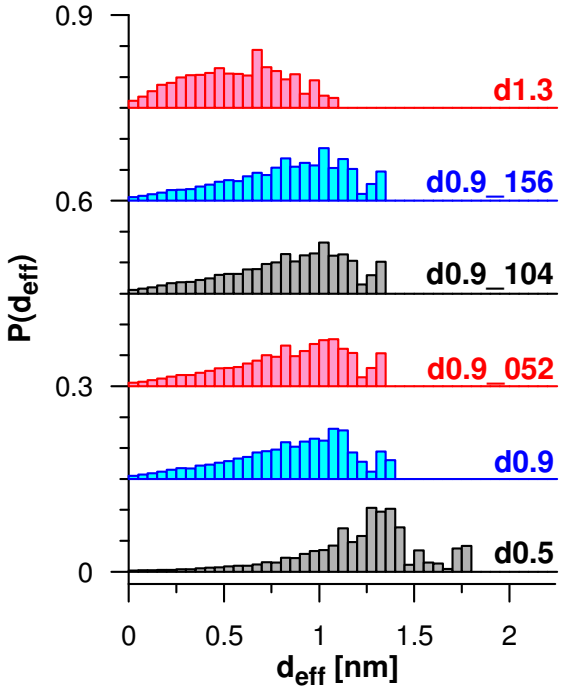

Figure 3. Comparison of the pore size histograms for all the considered VPCs (subsequent histograms were shifted by 0.15 from the previous ones).

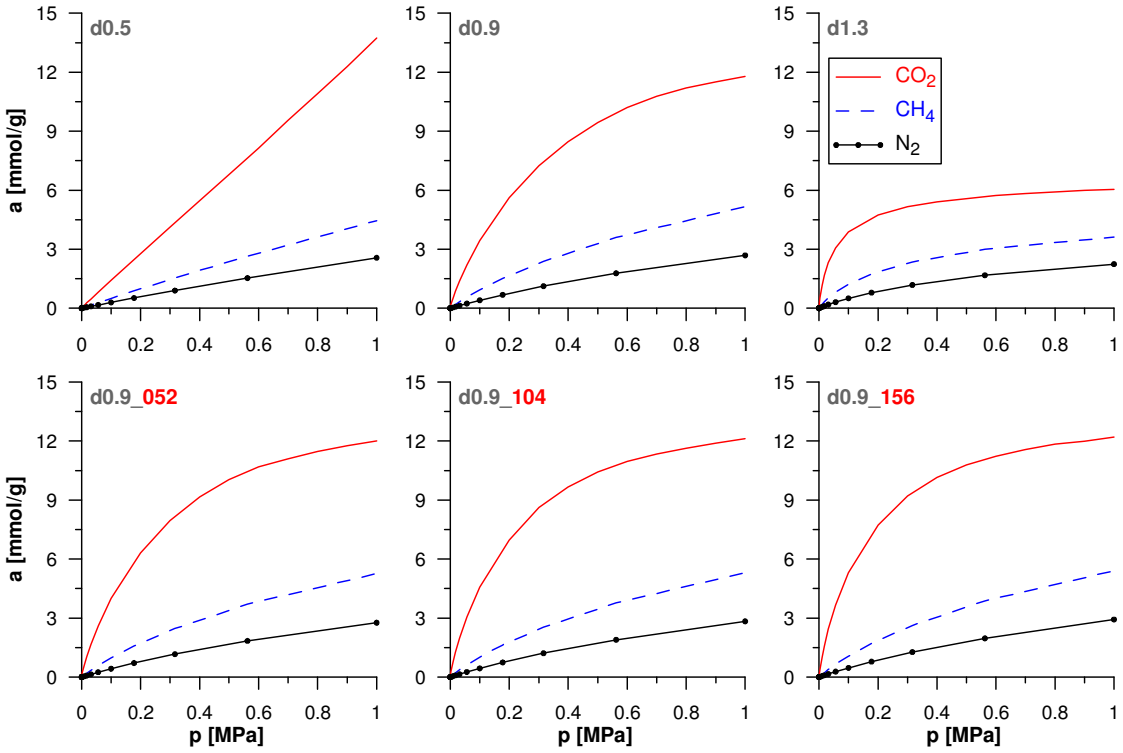

Figure 4. Comparison of single component CO_2, CH_4 or N_2 adsorption isotherms on all the considered VPCs (T = 298 K). Only the regions for pressure up to 1 MPa are shown.

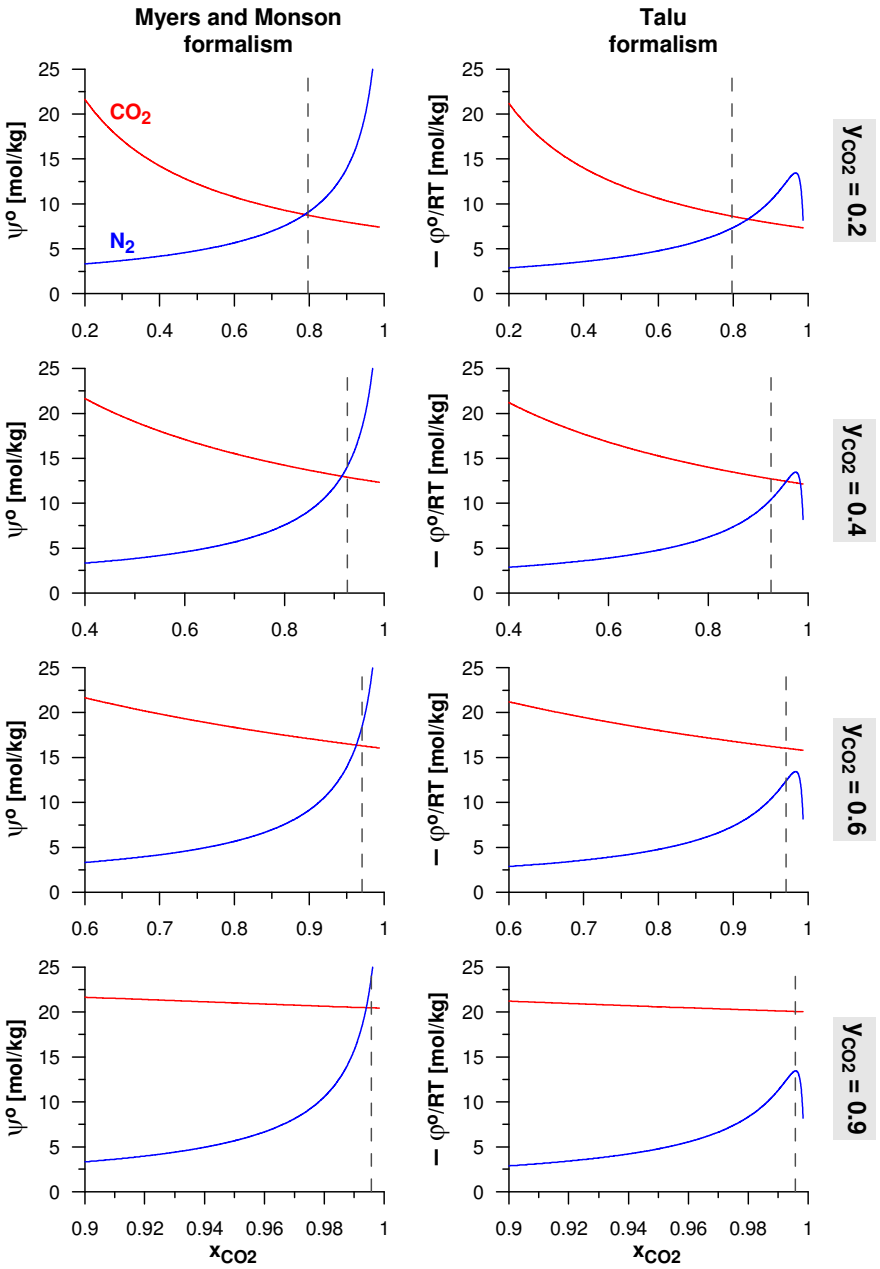

Figure 5. Visualisation of x_{CO2} finding according to the IAS theory – searching of equality $\psi_1^o = \psi_2^o$ (Myers and Monson formalism) or $\varphi_1^o = \varphi_2^o$ (Talu formalism) on the example of d0.9 carbon and CO_2/N_2 mixture at p_{tot} = 1 MPa and for selected y_{CO2} values. The vertical dashed lines present x_{CO2} value obtained for the simulation mixture adsorption. The grand potentials (ψ^o (Eq. (16)) and φ^o (Eq. (8)) are calculated for hypothetical values of CO_2 mole fractions in adsorbed phase (x_{CO2}) – formally $p_{CO2}^o = p_{tot} y_{CO2}/x_{CO2}$ and $p_{N2}^o = p_{tot}(1-y_{CO2})/(1-x_{CO2})$ (Eq. (17) for γ_i = 1). The curves are plotted for x_{CO2} range corresponds to the range of pressure simulated for single components adsorption (i.e. $p_{CO2}^o \le 1$ MPa and $p_{N2}^o \le 60$ MPa).

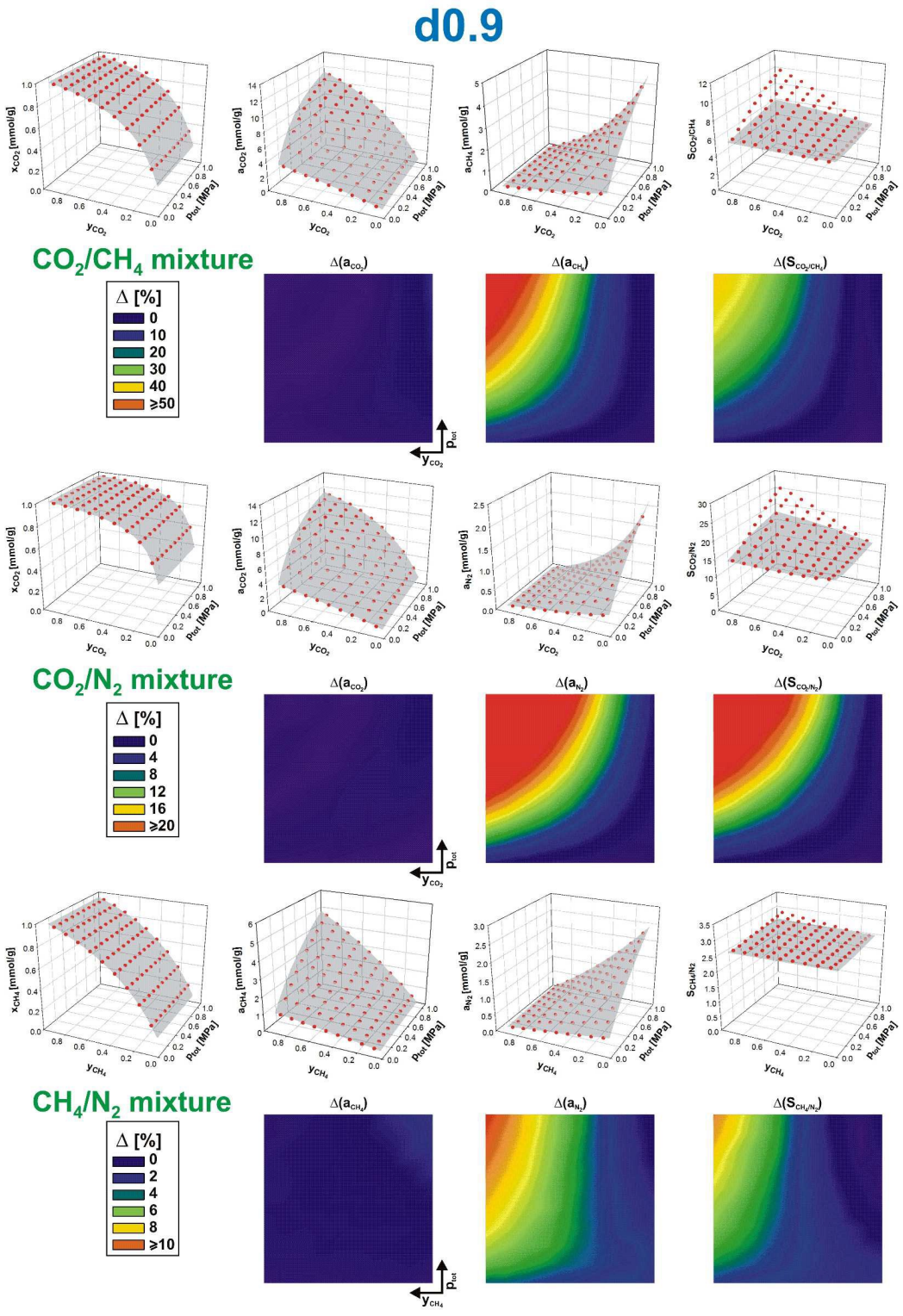

Figure 6. Comparison of the results simulated directly for ale the considered gas mixtures (points) and the predictions of IAS theory (planes) for the d0.9 carbon. The maps of the relative errors (Δ – Eq. (24)) for the values of component adsorption amounts ($\Delta(a_i)$) and equilibrium separation factors ($\Delta(S_{1/2})$) obtained from the IAS theory.

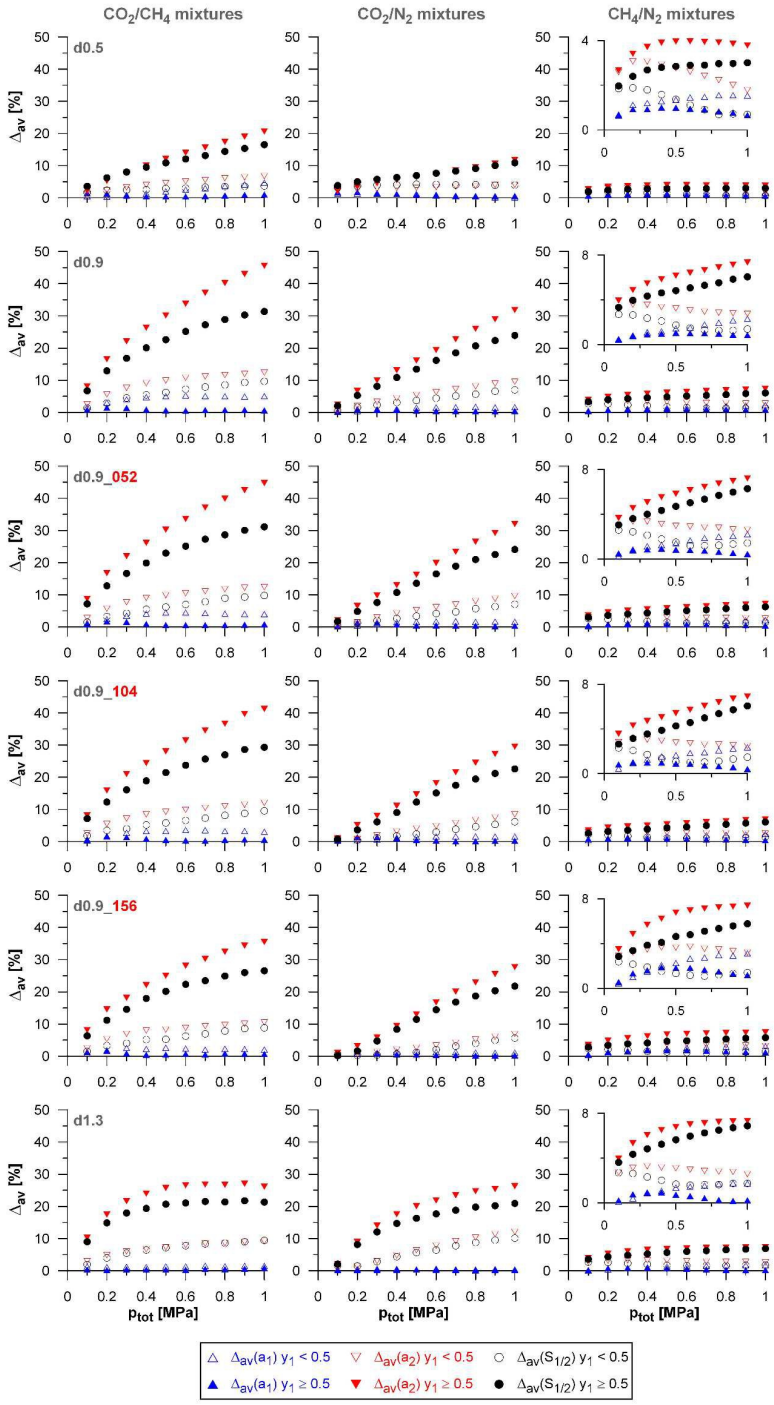

Figure 7. Comparison of the average relative errors (Δ_{av}) in the values of: (i) mixture components adsorption amounts (a_1 – blue and a_2 – red) and equilibrium separation factors ($S_{1/2}$ – black) calculated from the IAS theory. The errors were averaged for each total pressure value in two groups: (i) for the mol fraction of the 1st component in gaseous phase (y_1) below 0.5 (open symbols) and (ii) for $y_1 \geq 0.5$ (full symbols). The 1st component is CO_2 for CO_2/CH_4 and CO_2/N_2 mixtures and CH_4 for CH_4/N_2 mixture.

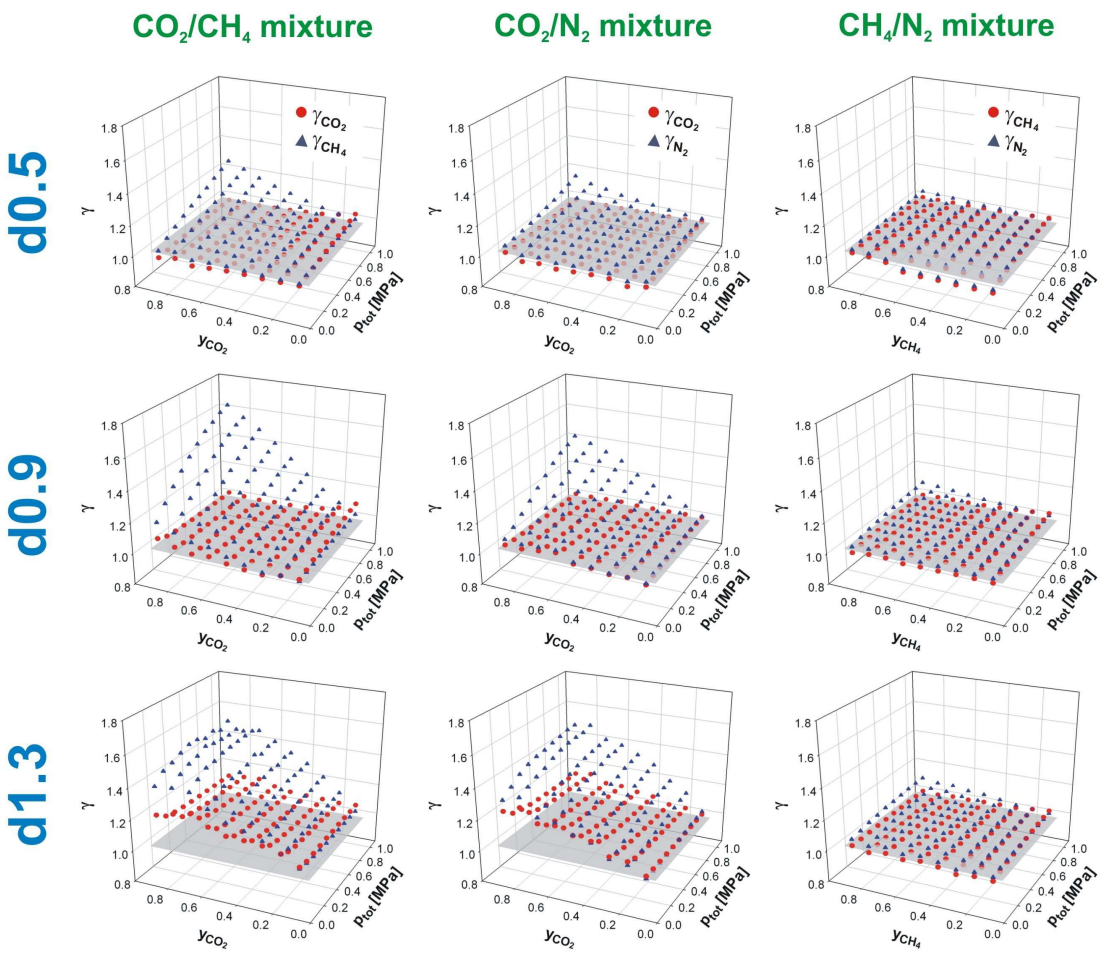

Figure 8. Comparison of calculated activity coefficients for mixture adsorption on unoxidised carbons. The grey planes represent $\gamma = 1$.

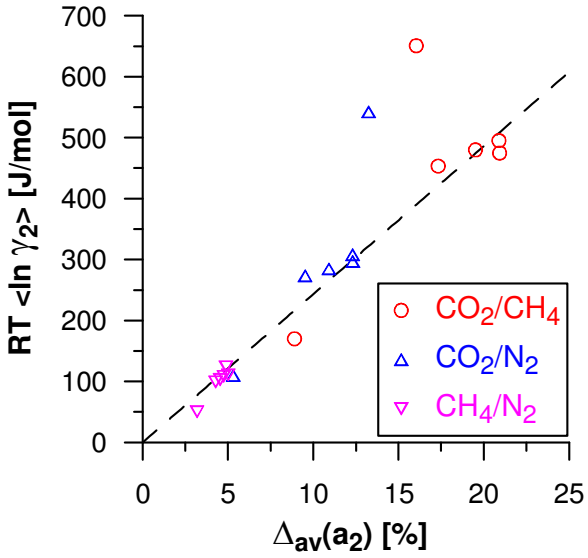

Figure 9. Dependence between the average relative errors for the values of the 2nd component adsorption amount predicted by IAS theory – $\Delta_{av}(a_2)$ (the data are averaged for all the considered simulation points) and average values of activity coefficients of this component in mixture (formally $RT \ln \gamma_2$). The dashed line was drawn to guide the eye.

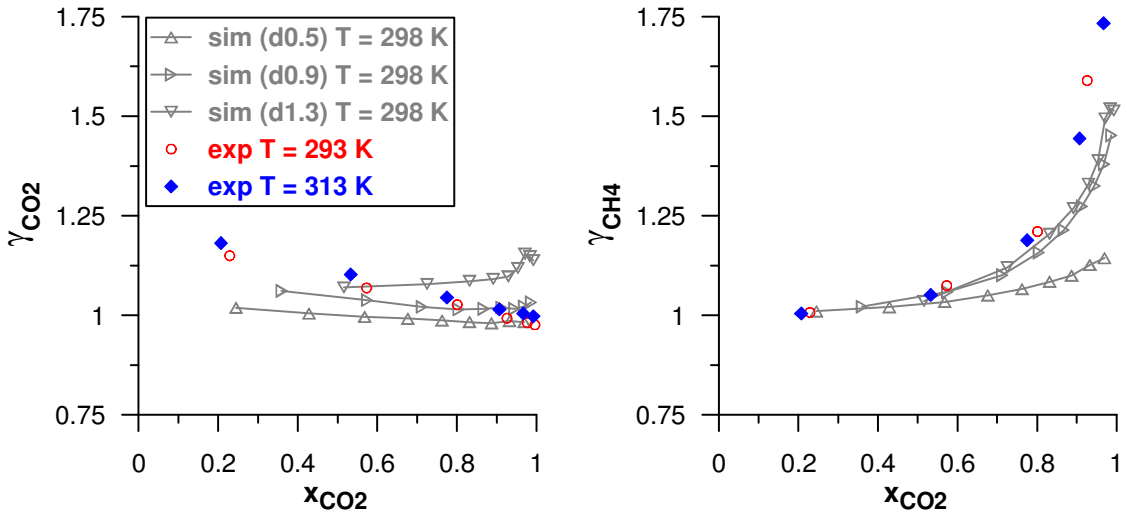

Figure 10. Comparison of activity coefficients of components for adsorption of CO_2/CH_4 mixture calculated using our simulation results for unoxidised carbons (at p_{tot} = 0.50 MPa and T = 298 K) and experimental data for A35/4 carbon[64] (at p_{tot} = 0.53 MPa and T = 293 K or T = 313 K).

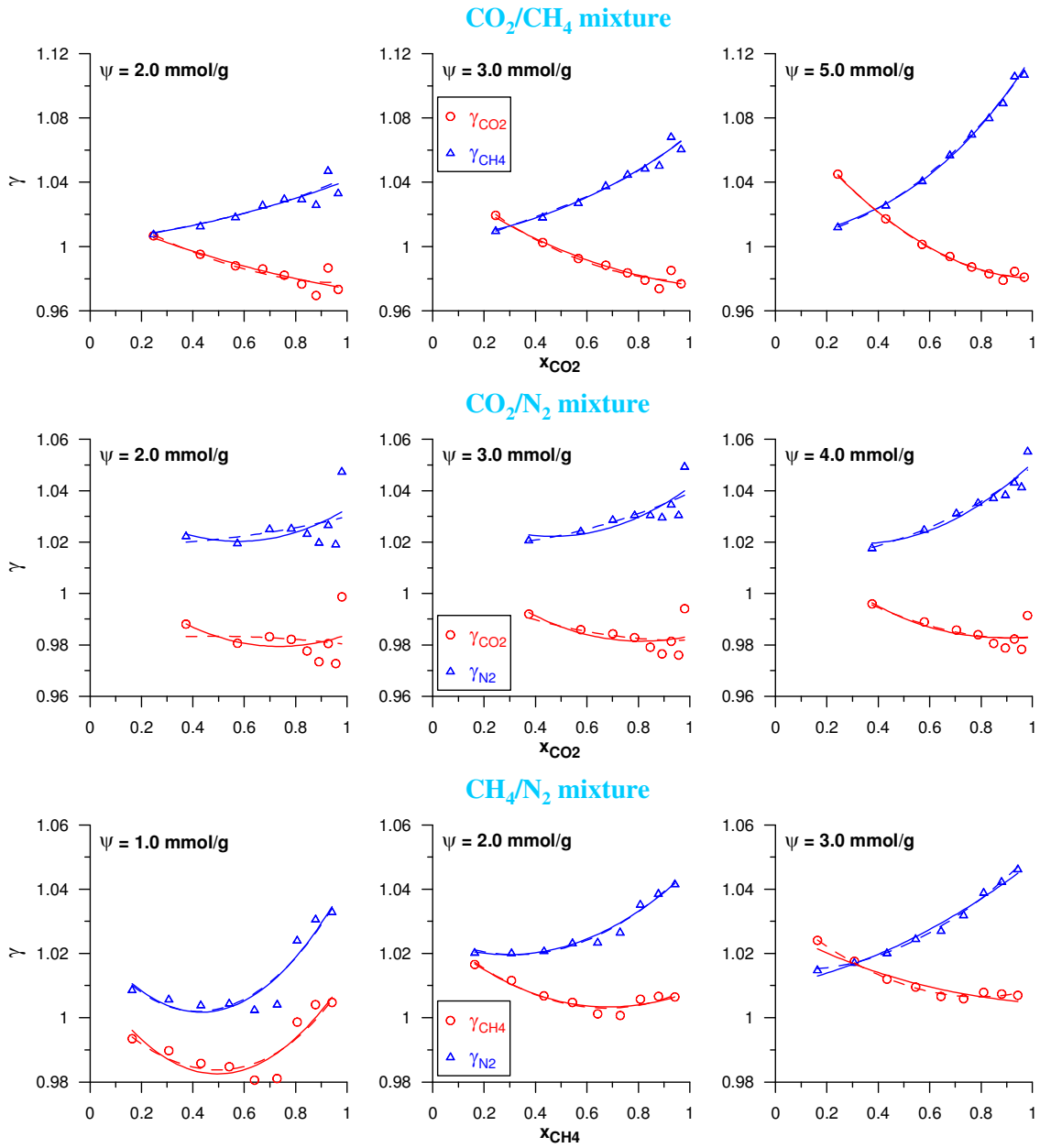

Figure 11. Comparison of the activity coefficients (plotted as the function of the mole fraction of the 1st component in the adsorbed phase) for adsorption of all the considered mixtures on the d0.5 carbon (arbitrarily chosen values of ψ are presented). The lines present approximation by theoretical models (solid lines – Eqs. (34) and (35), dashed lines – Eq. (36)).

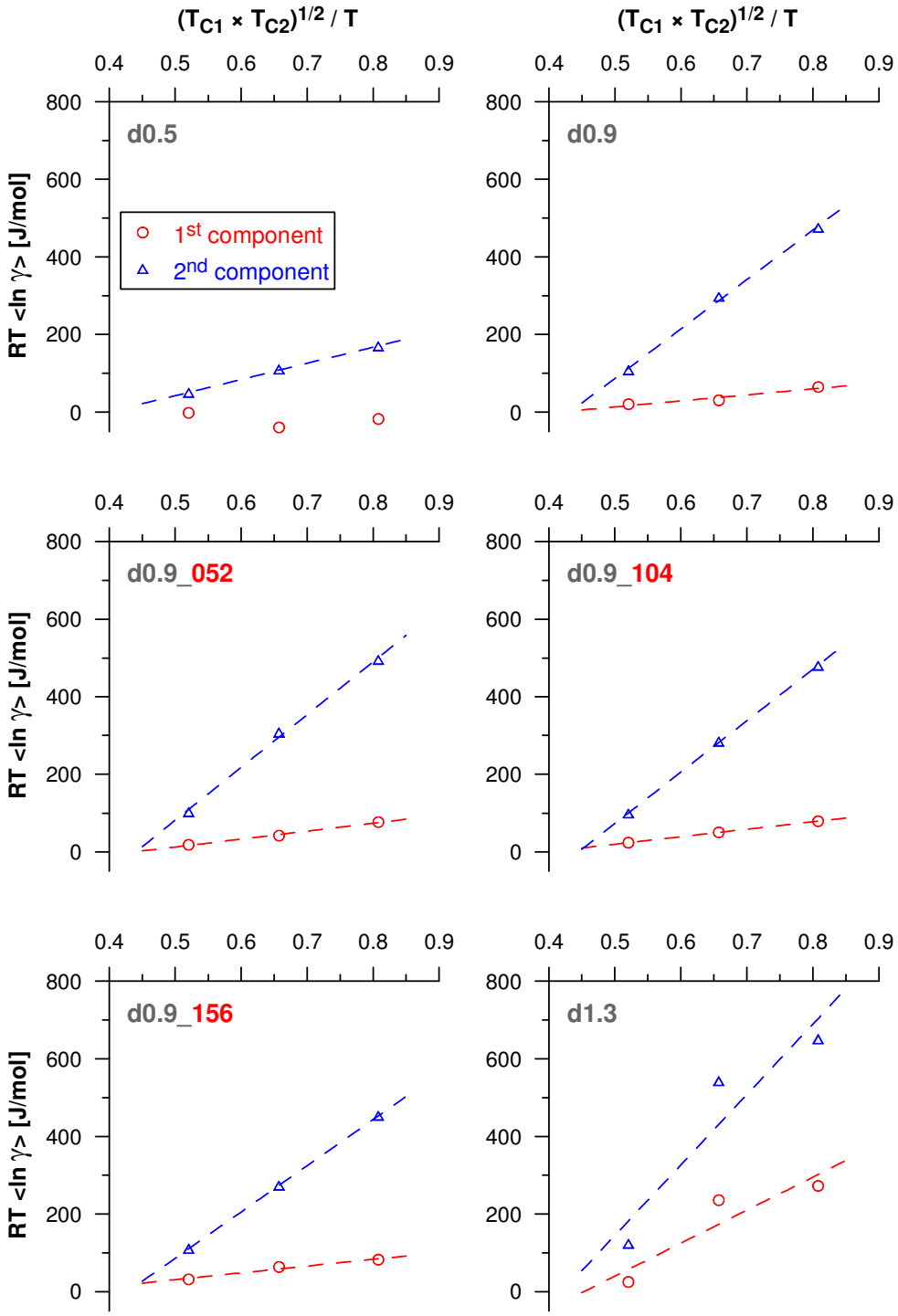

Figure 12. Correlations between average values of activity coefficients (formally $RT \ln \gamma$) and critical temperatures (T_{C1} and T_{C2}) for mixture components for all the considered carbons. T = 298 K is the temperature of simulation. 1st component is CO_2 for CO_2/CH_4 and CO_2/N_2 mixtures and CH_4 for CH_4/N_2 mixture. The dashed lines were drawn to guide the eye.